

Noise-induced entanglement transition in one-dimensional random quantum circuits

Qi Zhang¹ and Guang-Ming Zhang^{1,2*}

¹State Key Laboratory of Low-Dimensional Quantum Physics and
Department of Physics, Tsinghua University, Beijing 100084, China.

²Frontier Science Center for Quantum Information, Beijing 100084, China.

(Dated: April 11, 2022)

The random quantum circuit is a minimally structured model to study the entanglement dynamics of many-body quantum systems. In this paper, we considered a one-dimensional quantum circuit with noisy Haar-random unitary gates using density matrix operator and tensor contraction methods. It is shown that the entanglement evolution of the random quantum circuits is properly characterized by the logarithmic entanglement negativity. By performing exact numerical calculations, we found that, as the physical error rate is decreased below a critical value $p_c \approx 0.056$, the logarithmic entanglement negativity changes from the area law to the volume law, giving rise to an entanglement transition. The critical exponent of the correlation length can be determined from the finite-size scaling analysis, revealing the universal dynamic property of the noisy intermediate-scale quantum devices.

Recently, random quantum circuits have attracted considerable attention both theoretically and experimentally [1–13], because it provides a minimally structured toy model to study the dynamics of chaotic quantum many-body systems. Due to the fact that the complicated probability distribution, it is available to achieve quantum supremacy in sampling problems, which is impossible to simulate on classical computers at a large scale with deep depth. The famous experimental demonstration has been succeeded by Google’s superconducting processor without any error correction, where the device contains 53 available qubits with 20 circuit depths[1]. In a related theoretical work[3], the quantum fidelity metrics of the random quantum circuit has been well-studied, and they simulated Google’s random quantum circuit with tensor network states but the fidelity of two-qubit gates can only reach 92%. On the other hand, the most important feature in the dynamic process of the quantum circuits, such as the quantum entanglement, is far less understood.

In the absence of physical noise, von Neumann entanglement entropy or Rényi entropy and the corresponding entanglement spectrum are well used to characterize the entanglement properties in quantum circuits[11]. It has been established that the usual non-unitary projective measurement may destroy the quantum entanglement in random quantum circuits, and an entanglement phase transition is induced from an area law phase to a volume law phase when the probability of measurements is decreased[14–22]. However, for the random quantum circuit with physical noise, it is a challenge to separate the classical correlation from the quantum entanglement, where the noise can thermalize the system as a mixed state. The usual quantum mutual information for the mixed states usually overestimates the classical correlation[23–26]. So a natural question is how to exclusively diagnose quantum correlations in the noisy random quantum circuits. In a related paper[9], the operator space entanglement entropy[27–29] was used to mea-

sure the entanglement of the circuit, and no entanglement transition was observed for the gate error rate $p \geq 0.06$.

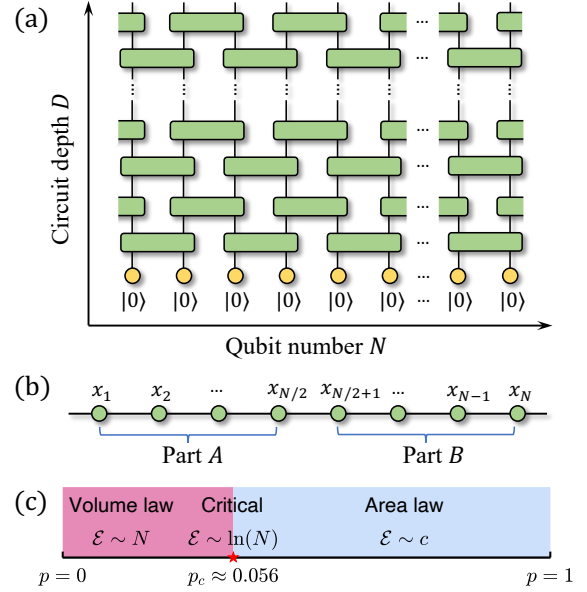


FIG. 1: (a) The sketch of a one-dimensional random quantum circuit contains N qubits and circuit depth D with periodic boundary conditions. The green rectangles are two-qubit Harr-random unitary operators with a gate error rate p . The yellow circles on the bottom indicate the input state, which is a pure product state. The output distribution can be obtained on the top of the circuit, which can be measured by the output string $|x_1, x_2, \dots, x_N\rangle$. (b) To compute the entanglement negativity, the output mixed state is divided into two parts A and B . (c) The entanglement transition driven by the physical noise p_c in the maximal logarithmic negativity separates the volume law and area law.

In this paper, we numerically simulate a one-dimensional quantum circuit with noisy Haar-random unitary gates through tensor contractions, as shown in Fig.1(a). We focus on the entanglement evolution of the

circuit with a lower error rate, because it is hard to accurately simulate at a large scale with tensor networks. We notice that the logarithmic entanglement negativity generated by the partial transpose (PT) density matrix [26, 30–38] can exclusively diagnose quantum correlations in noisy quantum circuits. The corresponding bipartition is shown in Fig.1(b). By analyzing the numerical results, we find an entanglement transition in the maximal logarithmic negativity from the area law to the volume law as the physical noise is decreased below a critical value $p_c \approx 0.056$, as shown in Fig.1(c). We also estimate the critical exponent of the correlation length $\nu \approx 1.25$, revealing the universal property of the noisy intermediate-scale quantum devices.

Noisy random quantum circuit. -Since the two-qubit gates can approach all operations in a random quantum circuit with a finite depth, we just consider the two-qubit gate to create the quantum correlation between two qubits. Specially, a two-qubit Haar-random unitary gate U with dimension $2^2 \times 2^2$ is applied to the system, and the unitary operation \mathcal{U} can be modeled by:

$$\mathcal{U}(\rho) = U\rho U^\dagger, \quad (1)$$

where ρ is the density matrix of the many-body system. In a 1D quantum circuit with N qubits and circuit depth D , we label the qubit from 1 to N , and the system starts from a pure product state, $|\Psi_0\rangle = |0\rangle^{\otimes N}$. In order to reduce the finite size effects, we use the periodic boundary conditions in our research. When the two-qubit unitary operations are applied, there are two kinds of patterns. For the odd circuit depth D , the two-qubit gates are just applied to the qubits with labeled $\{l, l+1\}$, ($l = 1, 3, 5, \dots$), while the two-qubit gates are applied to the qubits with labeled $\{l+1, l+2\}$, ($l = 1, 3, 5, \dots$) and $\{N, 1\}$ for the even circuit depth D . After a finite depth of two-qubit operations, the output state can be measured by the density matrix,

$$\rho = \sum_{ij} q_{ij} |\Psi_i\rangle \langle \Psi_j|, \quad (2)$$

where the diagonal terms q_{ii} are the probability of the basis state $|\Psi_i\rangle$. This resulting many-body state can be measured by an N -qubit string on the orthogonal basis:

$$|\Psi_i\rangle = |x_1, x_2, \dots, x_N\rangle \in \{|0\rangle, |1\rangle\}^{\otimes N}. \quad (3)$$

Then the probability of each basis state $|\Psi_i\rangle$ is obtained $q_{ii} = \langle \Psi_i | \rho | \Psi_i \rangle$, and the total probability satisfies $\text{Tr}(\rho) = \sum_i q_{ii} = 1$. Moreover, for a large circuit depth, the output state converges to a pure N -qubit Haar-random state, the so-called Page state[9, 39].

However, the operations on two-qubit gates cannot be completely accurate due to the presence of several kinds of physical noise in quantum circuits. The output state is a mixed state and is represented by the density matrix

ρ . To make the study more concrete, we consider the depolarization noise, which can be expressed as:

$$\mathcal{W}(\rho) = (1-p)\rho + \frac{p}{15} \sum_W W\rho W, \quad (4)$$

where the operator W belongs to the set of 15 non-trivial two-qubit Pauli operators $W \in \{I, X, Y, Z\}^{\otimes 2}$, and each type of noise occurs with equal probability $p/15$. It should be noticed that the operation \mathcal{W} is not unitary because of the summation, while each operator W is also Hermitian. The operations of two-qubit gates can be viewed as completely positive trace-preserving (CPTP) maps[9, 40],

$$\mathcal{M}(\rho) = \mathcal{U}(\rho) \circ \mathcal{W}(\rho), \quad (5)$$

where the trace of the density matrix is preserved under the operation. The physical meaning of each noisy Haar-random unitary gate is clear: the quantum entanglement between two qubits is generated under the operation \mathcal{U} , while the operation \mathcal{W} destroy the quantum coherence. Hence, the quantum entanglement in such a system will first grow up to a maximal and then decrease as the dynamic evolution. In the large circuit depth limit, the whole system will converge to a completely and globally depolarized state without any quantum entanglement, corresponding to the density identity matrix.

Entanglement negativity. -In the noisy quantum circuit, the system under the evolution is characterized by a mixed state. To describe the entanglement, we divide the system $|\Psi\rangle$ into two parts A and B , and mainly discuss the bipartite entanglement between them. The mixed state should be described by the density matrix ρ , rather than the wave function. In the Hilbert space, the density matrix ρ can be written in an orthogonal product basis,

$$\rho = \sum_{ijkl} \rho_{ijkl} |\psi_A^{(i)}, \psi_B^{(j)}\rangle \langle \psi_A^{(k)}, \psi_B^{(l)}|. \quad (6)$$

In order to describe the mixed state entanglement, we introduce the partial transpose (PT) density matrix,

$$\rho^{TA} = \sum_{ijkl} \rho_{ijkl} |\psi_A^{(k)}, \psi_B^{(j)}\rangle \langle \psi_A^{(i)}, \psi_B^{(l)}|, \quad (7)$$

which is defined by exchanging the physical indices of part A .

Moreover, the PT operation is a trace-preserving map, which ensures the eigenvalues λ_i of ρ^{TA} are real. Because it is not a completely positive map, the eigenvalues of ρ^{TA} may contain negative ones, and the existence of the negative eigenvalues is an indicator of quantum correlations of the mixed state. The negativity can be defined by[30–35]:

$$\mathcal{N} \equiv \frac{\|\rho^{TA}\|_1 - 1}{2} = \sum_{\lambda_i < 0} |\lambda_i|, \quad (8)$$

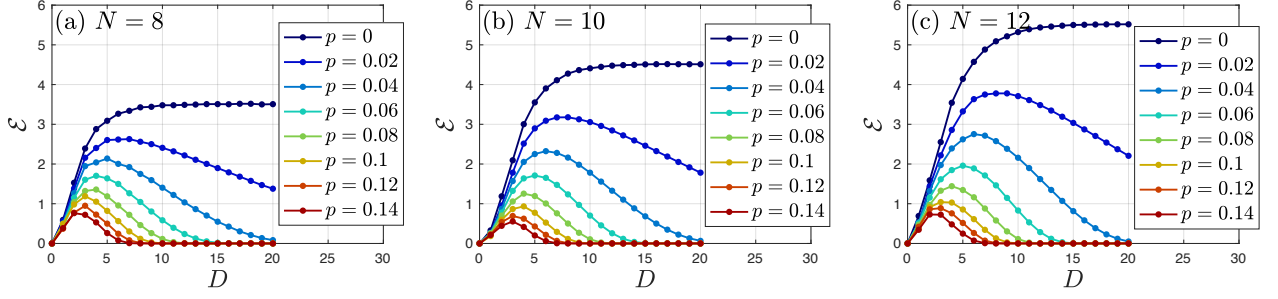


FIG. 2: The logarithmic negativity \mathcal{E} of the random quantum circuit. The lines with different colors correspond to various gate error rates p . The subsystem sizes of two parts are taken as $N_A = N_B = N/2$, the total system size is taken as (a) $N = 8$, (b) $N = 10$, (c) $N = 12$.

where $\|O\|_1 = \text{Tr}\sqrt{OO^\dagger}$ is the trace norm, i.e., the sum of the absolute value of the Hermitian matrix eigenvalues. Because the trace of the PT density matrix is preserved $\text{Tr}(\rho^{T_A}) = 1$, we can conclude that the above negativity \mathcal{N} is the sum of the absolute value of negative eigenvalues. If $\mathcal{N} > 0$, the well-known positive partial transpose (PPT) condition is violated, which indicates that part A and B must be entangled[34]. Although the PPT condition is not sufficient[31], the entanglement which can not be detected by the negativity may not be useful. So the negativity sets an upper bound on the distillable entanglement[34]. For convenience, the logarithmic negativity is usually defined by:

$$\mathcal{E} \equiv \log_2 \|\rho^{T_A}\|_1 = \log_2(2\mathcal{N} + 1). \quad (9)$$

Tensor network contraction is a powerful tool to simulate random quantum circuits, especially for quantum circuits with low quantum entanglement or shallow circuit depth[3, 12, 13]. However, for the high quantum entanglement system, the corresponding state cannot be accurately described by the matrix product state or matrix product operator with small bond dimensions[3, 41–46]. In the present study, the quantum circuits with physical noise ($p > 0$) are mixed states, and they should be simulated with density matrices in the whole space with dimension 2^{2N} . Due to the high computational cost of density matrix and entanglement negativity, we simulate a one-dimensional noisy random quantum circuit chain up to $N = 14$ qubits in the periodic boundary condition. In order to compute the logarithmic entanglement negativity of the system, the output mixed state should be divided into two parts A and B with equal sizes $N_A = N_B = N/2$, as shown in Fig.1(b).

Numerical results. -In Fig.2, we showed that the logarithmic entanglement negativity \mathcal{E} changes as increasing the circuit depth D for different system sizes N and various gate error rates p . Due to the randomness of the quantum circuit, we repeated over 50 times for the random samples and obtained the average logarithmic negativity.

In the absence of noise $p = 0$, as increasing the circuit depth D , the logarithmic negativity \mathcal{E} first grows linearly and then converges to a fixed value \mathcal{E}_{\max} . The circuit depth D corresponding to the entanglement saturation grows with the number of qubits N , and the circuit depth is proportional to the qubit number $D \sim N$, i.e., the logarithmic negativity \mathcal{E} can be regarded as a function of D/N . Since the whole circuit converges to an N -qubit Haar-random state, the logarithmic negativity can be expressed as $\mathcal{E}_{\max} = N/2 + c_1$, implying that the logarithmic negativity satisfied the volume law[26, 38].

In the presence of physical noise $p > 0$, the logarithmic negativity \mathcal{E} grows at first and then decreases. No matter how small the noise is, the logarithmic negativity finally vanishes in the large circuit depth limit. This is not surprising, because the system finally converges to a globally depolarized state without any entanglement. In the dynamic process of the circuit, we are most interested in the maximal achievable entanglement and the scaling law for the maximal logarithmic negativity \mathcal{E}_{\max} .

Let us consider a small gate error rate, such as $p = 0.02$. As the system size N grows, we can see the maximal logarithmic negativity \mathcal{E}_{\max} as a linear function of the circuit depth D increases, following the entanglement volume law. But when the gate error rate is quite large, such as $p = 0.14$, it is obvious that the evolution curves for various system sizes are almost the same, implying that the maximal logarithmic negativity \mathcal{E}_{\max} is independent of the system size N , corresponding to an area law entanglement. Hence, the scaling law of the maximal logarithmic negativity changes with increasing the gate error rate, and there is an entanglement transition between these two kinds of scaling law.

Entanglement transition. -To further analyze the scaling law of entanglement in the noisy random quantum circuit, we choose the number of quantum bits N as the horizontal axis and the maximal logarithmic negativity \mathcal{E}_{\max} of each circuit evolution as the vertical axis, and then connect the points with the same gate error rate p . The resulting scaling law is shown in Fig.3(a). It is clear

that, when the error rate p is small, the maximal logarithmic negativity \mathcal{E}_{\max} grows linearly with the system size N , which corresponds to the volume law entanglement. Also, we fit the maximal logarithmic negativity \mathcal{E}_{\max} in the noiseless case $p = 0$, and then obtain the fitting formula $\mathcal{E}_{\max} = 0.5001N - 0.4813$, which is consistent with the previous analytical result[26, 38]. When the gate error rate is large, such as $p = 0.14$, the maximal logarithmic negativity \mathcal{E}_{\max} does not increase with the system size N growing, which indicates the entanglement area law. Due to the finite size effect and the oddity of subsystems A and B , the curves slightly oscillate with various system sizes. There should be a critical point between the area law and the volume law entanglement, which may satisfy the $\log(N)$ correction.

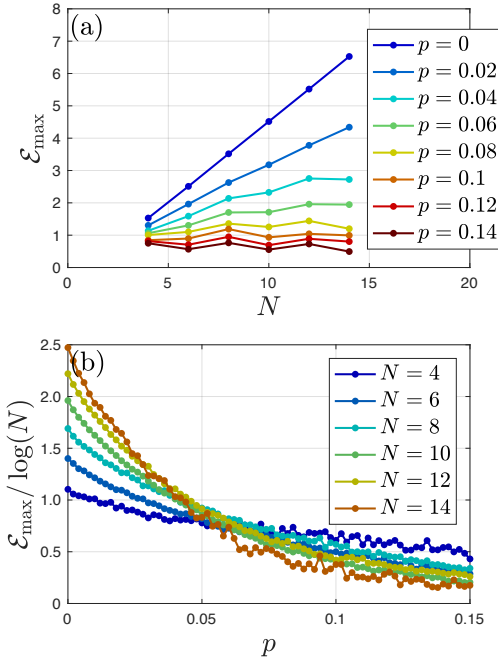


FIG. 3: (a) The maximal logarithmic negativity \mathcal{E}_{\max} changes as a function of the system size N , where all the numerical results are taken with subsystem size $N_A = N_B = N/2$. (b) The maximal logarithmic negativity is divided by the logarithmic of the system size $\mathcal{E}_{\max} / \log(N)$ versus gate error rate p , where the entanglement negativities collapse together around the critical point $p_c \approx 0.056$.

In the following, when dividing the maximal logarithmic negativity by the logarithm of the system size $\mathcal{E}_{\max} / \log(N)$, we consider its change as a function of the gate error rate p . Because the numerical results of different system sizes collapse together, we can get the entanglement phase transition point p_c . As shown in Fig.3(b), all the curves almost overlap at around $p_c \approx 0.056$. Above the critical point, the maximal logarithmic negativity satisfies $\mathcal{E}_{\max} \sim \log(N)$. For $p < p_c$, the scaling law of entanglement is stronger than the $\log(N)$ correc-

tion, entering into the volume law phase. In contrast, when $p > p_c$, $\mathcal{E}_{\max} / \log(N)$ decreases as the system size increases. Eventually, it will converge to zero in the thermodynamic limit $N \rightarrow \infty$. Therefore, the phase diagram can be established, as shown in Fig.1(a).

To further study the entanglement scaling law, we can extract a critical exponent. Since the maximal logarithmic negativity divided by the logarithmic of the system size $\mathcal{E}_{\max} / \log(N)$ can be viewed as a function of the gate error rate p and the size of the system N , we employ the following hypothesis,

$$\mathcal{E}_{\max} / \ln(N) \sim f\left((p - p_c)N^{1/\nu}\right), \quad (10)$$

where $f(x)$ is a universal function and ν is the correlation length exponent. As shown in Fig.4, all the points have an excellent collapse with $\nu \approx 1.25$. On the right side of the graph, it is the region satisfied the area law entanglement, and we find the systems with $N = 4, 8, 12$ and $N = 6, 10, 14$ collapse better with each other due to the oddity of the subsystem. It should be mentioned that both critical point position and critical exponent are related to the entanglement measure[14, 17]. It is interesting that our numerical value is similar to the projective measure induced transition in random quantum circuits, where through the tripartite mutual information the correlation length exponent is $\nu \approx 1.22$ for the circuit consisting of the Haar-random gate[17].

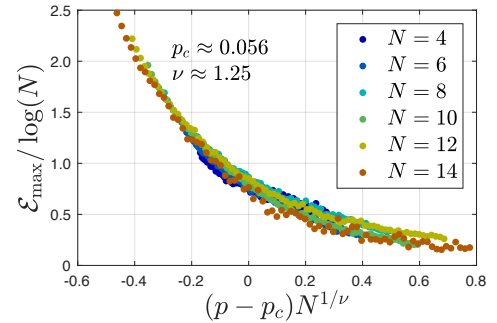


FIG. 4: The maximal logarithmic negativity is divided by the logarithmic of the system size $\mathcal{E}_{\max} / \log(N)$, which changes as a function of $(p - p_c)N^{1/\nu}$, where the critical point is taken as $p_c \approx 0.056$. The correlation length exponent $\nu \approx 1.25$ for the best collapse.

Discussions and Conclusions. -It should be noticed that the random quantum circuits in the experiments[1, 2, 5] have used different qubit gates, each circuit depth usually consists of one layer fixed two-qubit gates, and one layer single-qubit gates randomly chosen from \sqrt{X} , \sqrt{Y} , and $\sqrt{X + Y}$. Our further numerical simulations have found that the dynamics in the circuits with two-qubit $\sqrt{\text{iSWAP}}$ gates are close to the Haar-random gates, where the critical point is around $p_c \approx 0.040$ with the critical exponent $\nu \approx 1.30$.

We would also like to point out that the usual correlated many-body systems are quite different from our random quantum circuits with high entanglement. In most cases, the ground states satisfy the area law entanglement, which can be described accurately by a small Hilbert space. And the large system sizes are required to derive the scaling behavior. However, when the whole Hilbert space is used to describe the random quantum circuits with the volume law entanglement, the circuit with a small number of qubits has already contained a huge Hilbert space, so the scaling behavior can be seen even in small systems. Hence, we believe that the noise-driven entanglement transition and its criticality found in this paper can be valid in large-scale systems. Similarly, for the projective measurement-driven entanglement transition[17], the results derived from the small size systems are comparable to the large sizes, indicating that the entanglement phase transition is universal.

Because both the physical noise and projective measurements destroy the quantum coherence of the system, the non-unitary projective measurement model has some similarities to the noisy in the random quantum circuits. In the projective measurement-driven quantum circuit, the system is always in the pure states and the entanglement grows as the circuit depth increases until saturating[14–22]. To measure the mixed state entanglement in the noisy random quantum circuits, however, we have to use the measure of logarithmic entanglement negativity, which can be measured experimentally through the PT moments[47]. More recently, quantum algorithms are also proposed to measure the entanglement negativity in noisy intermediate-scale quantum devices[48].

In conclusion, we have simulated the noisy random quantum circuits with density matrix operators and tensor contractions, and characterized the mixed state entanglement through the logarithmic entanglement negativity. With the decreasing gate error rate, we have found that the scaling law of the maximal logarithmic negativity changes from the area law to the volume law. Between these two phases, the critical point has determined as $p_c \approx 0.056$ and a correlation length exponent has also been estimated $\nu \approx 1.25$. These results not only reveal the dynamics in chaotic quantum many-body systems, but also are valuable for designing noisy intermediate-scale quantum devices.

Acknowledgement. -The authors acknowledge the stimulating discussions with Lei Wang and Tao Xiang, and the research is supported by the National Key Research and Development Program of MOST of China (2017YFA0302902).

* Electronic address: gmzhang@tsinghua.edu.cn

[1] F. Arute, K. Arya, R. Babbush, D. Bacon, J. C. Bardin,

- R. Barends, R. Biswas, S. Boixo, F. G. S. L. Brandao, D. A. Buell, et al., *Nature* **574**, 505 (2019), URL <https://doi.org/10.1038/s41586-019-1666-5>.
- [2] Y. Wu, W.-S. Bao, S. Cao, F. Chen, M.-C. Chen, X. Chen, T.-H. Chung, H. Deng, Y. Du, D. Fan, et al., *Phys. Rev. Lett.* **127**, 180501 (2021), URL <https://link.aps.org/doi/10.1103/PhysRevLett.127.180501>.
- [3] Y. Zhou, E. M. Stoudenmire, and X. Waintal, *Phys. Rev. X* **10**, 041038 (2020), URL <https://link.aps.org/doi/10.1103/PhysRevX.10.041038>.
- [4] A. Nahum, S. Vijay, and J. Haah, *Phys. Rev. X* **8**, 021014 (2018), URL <https://link.aps.org/doi/10.1103/PhysRevX.8.021014>.
- [5] X. Mi, P. Roushan, C. Quintana, S. Mandrà, J. Marshall, C. Neill, F. Arute, K. Arya, J. Atalaya, R. Babbush, et al., *Science* **374**, 1479 (2021), <https://www.science.org/doi/pdf/10.1126/science.abg5029>, URL <https://www.science.org/doi/abs/10.1126/science.abg5029>.
- [6] S. Xu and B. Swingle, *Nature Physics* **16**, 199 (2020), URL <https://doi.org/10.1038/s41567-019-0712-4>.
- [7] S. Boixo, S. V. Isakov, V. N. Smelyanskiy, R. Babbush, N. Ding, Z. Jiang, M. J. Bremner, J. M. Martinis, and H. Neven, *Nature Physics* **14**, 595 (2018), URL <https://doi.org/10.1038/s41567-018-0124-x>.
- [8] C. Neill, P. Roushan, K. Kechedzhi, S. Boixo, S. V. Isakov, V. Smelyanskiy, A. Megrant, B. Chiaro, A. Dunsworth, K. Arya, et al., *Science* **360**, 1957199 (2018), ISSN 1095-9203, URL <http://dx.doi.org/10.1126/science.aao4309>.
- [9] K. Noh, L. Jiang, and B. Fefferman, *Quantum* **4**, 318 (2020), ISSN 2521-327X, URL <https://doi.org/10.22331/q-2020-09-11-318>.
- [10] S. Cheng, C. Cao, C. Zhang, Y. Liu, S.-Y. Hou, P. Xu, and B. Zeng, *Phys. Rev. Research* **3**, 023005 (2021), URL <https://link.aps.org/doi/10.1103/PhysRevResearch.3.023005>.
- [11] A. Nahum, J. Ruhman, S. Vijay, and J. Haah, *Phys. Rev. X* **7**, 031016 (2017), URL <https://link.aps.org/doi/10.1103/PhysRevX.7.031016>.
- [12] J. Napp, R. L. La Placa, A. M. Dalzell, F. G. S. L. Brandao, and A. W. Harrow, arXiv e-prints arXiv:2001.00021 (2019), 2001.00021.
- [13] I. L. Markov and Y. Shi, *SIAM Journal on Computing* **38**, 963–981 (2008), ISSN 1095-7111, URL <http://dx.doi.org/10.1137/050644756>.
- [14] Y. Li, X. Chen, and M. P. A. Fisher, *Phys. Rev. B* **98**, 205136 (2018), URL <https://link.aps.org/doi/10.1103/PhysRevB.98.205136>.
- [15] B. Skinner, J. Ruhman, and A. Nahum, *Phys. Rev. X* **9**, 031009 (2019), URL <https://link.aps.org/doi/10.1103/PhysRevX.9.031009>.
- [16] Y. Bao, S. Choi, and E. Altman, *Phys. Rev. B* **101**, 104301 (2020), URL <https://link.aps.org/doi/10.1103/PhysRevB.101.104301>.
- [17] A. Zabalo, M. J. Gullans, J. H. Wilson, S. Gopalakrishnan, D. A. Huse, and J. H. Pixley, *Phys. Rev. B* **101**, 060301 (2020), URL <https://link.aps.org/doi/10.1103/PhysRevB.101.060301>.
- [18] S. Choi, Y. Bao, X.-L. Qi, and E. Altman, *Phys. Rev. Lett.* **125**, 030505 (2020), URL <https://link.aps.org/doi/10.1103/PhysRevLett.125.030505>.
- [19] O. Lunt, J. Richter, and A. Pal, arXiv e-prints arXiv:2112.06682 (2021), 2112.06682.

- [20] S. Sang and T. H. Hsieh, Phys. Rev. Research **3**, 023200 (2021), URL <https://link.aps.org/doi/10.1103/PhysRevResearch.3.023200>.
- [21] A. Lavasani, Y. Alavirad, and M. Barkeshli, Nature Physics **17**, 342 (2021), URL <https://doi.org/10.1038/s41567-020-01112-z>.
- [22] Y. Li and M. P. A. Fisher, Phys. Rev. B **103**, 104306 (2021), URL <https://link.aps.org/doi/10.1103/PhysRevB.103.104306>.
- [23] C. Adami and N. J. Cerf, Phys. Rev. A **56**, 3470 (1997), URL <https://link.aps.org/doi/10.1103/PhysRevA.56.3470>.
- [24] B. Groisman, S. Popescu, and A. Winter, Phys. Rev. A **72**, 032317 (2005), URL <https://link.aps.org/doi/10.1103/PhysRevA.72.032317>.
- [25] M. Žnidarič, T. c. v. Prosen, and I. Pižorn, Phys. Rev. A **78**, 022103 (2008), URL <https://link.aps.org/doi/10.1103/PhysRevA.78.022103>.
- [26] H. Shapourian, S. Liu, J. Kudler-Flam, and A. Vishwanath, PRX Quantum **2** (2021), ISSN 2691-3399, URL <http://dx.doi.org/10.1103/PRXQuantum.2.030347>.
- [27] P. Zanardi, Phys. Rev. A **63**, 040304 (2001), URL <https://link.aps.org/doi/10.1103/PhysRevA.63.040304>.
- [28] T. c. v. Prosen and I. Pižorn, Phys. Rev. A **76**, 032316 (2007), URL <https://link.aps.org/doi/10.1103/PhysRevA.76.032316>.
- [29] V. Alba, J. Dubail, and M. Medenjak, Phys. Rev. Lett. **122**, 250603 (2019), URL <https://link.aps.org/doi/10.1103/PhysRevLett.122.250603>.
- [30] A. Peres, Phys. Rev. Lett. **77**, 1413 (1996), URL <https://link.aps.org/doi/10.1103/PhysRevLett.77.1413>.
- [31] M. Horodecki, P. Horodecki, and R. Horodecki, Physics Letters A **223**, 1–8 (1996), ISSN 0375-9601, URL [http://dx.doi.org/10.1016/S0375-9601\(96\)00706-2](http://dx.doi.org/10.1016/S0375-9601(96)00706-2).
- [32] K. Życzkowski, P. Horodecki, A. Sanpera, and M. Lewenstein, Phys. Rev. A **58**, 883 (1998), URL <https://link.aps.org/doi/10.1103/PhysRevA.58.883>.
- [33] J. Eisert and M. B. Plenio, Journal of Modern Optics **46**, 145–154 (1999), ISSN 1362-3044, URL <http://dx.doi.org/10.1080/09500349908231260>.
- [34] G. Vidal and R. F. Werner, Phys. Rev. A **65**, 032314 (2002), URL <https://link.aps.org/doi/10.1103/PhysRevA.65.032314>.
- [35] M. B. Plenio, Phys. Rev. Lett. **95**, 090503 (2005), URL <https://link.aps.org/doi/10.1103/PhysRevLett.95.090503>.
- [36] P. Ruggiero, V. Alba, and P. Calabrese, Phys. Rev. B **94**, 195121 (2016), URL <https://link.aps.org/doi/10.1103/PhysRevB.94.195121>.
- [37] H. Shapourian, P. Ruggiero, S. Ryu, and P. Calabrese, SciPost Phys. **7**, 37 (2019), URL <https://scipost.org/10.21468/SciPostPhys.7.3.037>.
- [38] J. Kudler-Flam, V. Narovlansky, and S. Ryu, arXiv e-prints arXiv:2109.02649 (2021), 2109.02649.
- [39] D. N. Page, Phys. Rev. Lett. **71**, 1291 (1993), URL <https://link.aps.org/doi/10.1103/PhysRevLett.71.1291>.
- [40] M.-D. Choi, Linear Algebra and its Applications **10**, 285 (1975), ISSN 0024-3795, URL <https://www.sciencedirect.com/science/article/pii/0024379575900750>.
- [41] G. Vidal, Phys. Rev. Lett. **91**, 147902 (2003), URL <https://link.aps.org/doi/10.1103/PhysRevLett.91.147902>.
- [42] F. Verstraete, J. J. García-Ripoll, and J. I. Cirac, Phys. Rev. Lett. **93**, 207204 (2004), URL <https://link.aps.org/doi/10.1103/PhysRevLett.93.207204>.
- [43] M. B. Hastings, Phys. Rev. B **73**, 085115 (2006), URL <https://link.aps.org/doi/10.1103/PhysRevB.73.085115>.
- [44] F. Verstraete, V. Murg, and J. Cirac, Advances in Physics **57**, 143 (2008), URL <https://doi.org/10.1080/14789940801912366>.
- [45] M. Zwolak and G. Vidal, Phys. Rev. Lett. **93**, 207205 (2004), URL <https://link.aps.org/doi/10.1103/PhysRevLett.93.207205>.
- [46] B. Pirvu, V. Murg, J. I. Cirac, and F. Verstraete, New Journal of Physics **12**, 025012 (2010), URL <https://doi.org/10.1088/1367-2630/12/2/025012>.
- [47] A. Elben, R. Kueng, H.-Y. R. Huang, R. van Bijnen, C. Kokail, M. Dalmonte, P. Calabrese, B. Kraus, J. Preskill, P. Zoller, et al., Phys. Rev. Lett. **125**, 200501 (2020), URL <https://link.aps.org/doi/10.1103/PhysRevLett.125.200501>.
- [48] K. Wang, Z. Song, X. Zhao, Z. Wang, and X. Wang, arXiv e-prints arXiv:2012.14311 (2020), 2012.14311.